Desalination and Water Treatment
www.deswater.com
doi: 10.1080/19443994.2015.1040463

57 (2016) 10894–10904
May

Taylor & Francis
Taylor & Francis Group

Experimental parameter optimization study on the acid leaching of coal fly ash

Long Yan[a,b,*], Junfei Shang[c], Yufei Wang[a,b], Jian Li[a,b], Huijin Liu[a,b], Tiantian Qu[a], Chao Zhang[a]

[a]*Yulin Engineering Research Center for Industrial Water Treatment, School of Chemistry and Chemical Engineering, Yulin University, Yulin 719000, China, Tel./Fax: +86 912 3896585; emails: ylyanlong@126.com (L. Yan), wangyufei0003@163.com (Y. Wang), lijian5220@163.com (J. Li), liuhuijing0205@sina.com (H. Liu), 1524679747@qq.com (T. Qu), 592412517@qq.com (C. Zhang)*

[b]*Shaanxi Key Laboratory of Low Metamorphic Coal Clean Utilization, Yulin University, Yulin 719000, China*

[c]*Shaanxi Yulin Excelle Coal Chemical Industry Co., Ltd., Yulin 719000, China, email: 00shangjunfei@163.com*

Received 22 September 2014; Accepted 7 April 2015

ABSTRACT

Coal fly ash from a power plant was leached using HCl. Factors that influenced the leaching process, such as the ratio of coal fly ash to Na_2CO_3, the HCl concentration, the leaching time, and the temperature, were investigated, and an orthogonal test was used to determine the optimal conditions for acid leaching the coal fly ash. The coal fly ash samples before and after acid leaching were analyzed by scanning electron microscopy, energy dispersive spectroscopy, and Brunauer–Emmett–Teller adsorption analysis. An aluminum leaching rate of 90.68% was obtained using the optimal values of 6 g Na_2CO_3, 100 g coal fly ash, 4 mol L^{-1} HCl, 1.5 h leaching time, and a temperature of 100°C. The concentrations of Al^{3+} and Fe^{2+} plus Fe^{3+} in the leaching liquid were 34.21 and 30.67 g L^{-1}, respectively, using the optimal conditions. The coal fly ash residue had certain specific surface area and absorption features that are described. The results suggest that acid leaching offers benefits in terms of the comprehensive use of coal fly ash.

Keywords: Coal fly ash; Acid leaching; Orthogonal test; Hydrochloric acid; Specific surface area

1. Introduction

The rapid growth of the power industry is closely related to the rapid growth of the industrial economy, and the generation of electricity in China mainly uses coal as a fuel [1,2]. In the powdered coal combustion process in a power plant, some non-combustible materials are first mixed with the injected air, and a high temperature flue gas is produced in which the non-combustible materials partially melt to form a large number of small spherical particles. These particles are captured by a dust collecting device as a gray–black coal fly ash, which is composed of small and light particles that are easily kept airborne by wind if they are released into the environment [3]. If coal fly ash is directly discharged into the environment, it may cause serious environmental problems, polluting water, the atmosphere, and soil, and the

*Corresponding author.

landscape in general [4]. Coal fly ash is one of the main industrial waste residues that are currently emitted in China. Traditionally, most coal fly ash has been dumped in landfills, but this could lead to harmful effects through future uses of the land and to problems maintaining the land [5]. There has been an increase in interest in making use of fly ash in recent years. Some coal fly ash is used in construction materials in civil engineering projects, but approximately 15% of coal ash is only recycled in any way globally [6]. The use of coal fly ash has, therefore, attracted widespread attention, and it has become an important subject in the field of environmental protection in terms of the comprehensive use of industrial waste residues.

Coal fly ash is rich in Si, Al, Fe, and other elements. However, these elements are present in the form of minerals with stable structures [7]. Si and Al are mainly present in the form of the mullite phase ($3Al_2O_3.2SiO_2$), in which the Si–Al bond is stable and not easily broken, meaning that Al is difficult to extract from coal fly ash using conventional methods [7–9]. In general, Al and Fe are abundant in an acid solution that has been used to leach coal ash, and they can be used to produce a coagulant for treating wastewater, the leached coal fly ash residue can also be used as an adsorbent, and this use allows the total environmental pollution caused by the solid waste from coal combustion to be mitigated and effectively add value using the coal fly ash productively [10–13]. Many researchers have performed studies on the leaching of elements from coal fly ash in recent years, but most leaching processes are still at the laboratory testing stage, and there have been few reports of leaching being used in industrial applications. The main problem that restricts the use of coal fly ash is achieving the efficient extraction of Al and Fe from the coal fly ash [14–16].

In the work presented here, hydrochloric acid was used to leach coal fly ash under reflux condensation. Yulin City is an important area for the energy and chemical industries in China, and a lot of coal fly ash is generated in this area in power plants. Excess hydrochloric acid is also produced in large amounts in factories in Yulin City, making this a convenient acid for leaching the coal fly ash produced in the area. We aimed to comprehensively and efficiently use these local resources, and the effects of the dosage of the activator Na_2CO_3 in a coal fly ash sample, the hydrochloric acid concentration, the reaction time, and the reaction temperature on the acid leaching process were studied separately. The optimal conditions for acid leaching coal fly ash were then determined using an orthogonal test. Finally, the coal fly ash samples before and after acid leaching were analyzed using scanning electron microscopy (SEM), energy dispersive spectroscopy (EDS), and Brunauer–Emmett–Teller adsorption (BET) analysis and the properties of the unleached and leached samples were compared.

2. Experimental details

2.1. Materials

Coal fly ash was collected from the Shenhua Guohua power plant in the Yulin Shenfu Economic Development Zone, Shaanxi Province, China. One of the seven largest coalfields in the world is located in this area. The chemical properties of the coal fly ash were determined by X-ray fluorescence analysis (XRF) by the coal fly ash supplier, and they are listed in Table 1. The coal fly ash was a typical silicon–aluminum coal fly ash, of a high quality, and it was rich in iron and deficient in calcium. Analytical reagent grade HCl and Na_2CO_3 were purchased from the Xi'an Reagent Co. (Xi'an, China), and all of the other reagents were purchased from the Tianjin Reagent Co. (Tianjin, China).

2.2. Experimental procedure

The coal fly ash samples were reacted with the HCl solution (300 mL) at a specified temperature in a 500-mL three-necked glass reactor vessel to which a straight condenser was connected (Fig. 1). The raw coal fly ash was mixed with Na_2CO_3 and the mixture was calcined at 800 °C for 2 h, then the mixture was treated with the HCl solution. The effects of using different weight ratios of the raw coal fly ash to Na_2CO_3, HCl concentrations, leaching temperatures, and leaching times were determined, but the calcination temperature and time were taken from the literature [17,18]. The yellow–green viscous liquid that was produced was suction filtered, washed until the washings had a pH of 7, and dried, then the acid-leached coal fly ash sample was prepared and analyzed by SEM, EDS, and BET. The Al^{3+} concentration in the leaching liquid was measured by replacement complexometric titration method (excess EDTA solution was added to chelate Al^{3+}, the free EDTA titrated with a standard zinc chloride solution) according to the Chinese national standard method and used as an index for investigating the effects of the different experimental conditions that were used [19]. Furthermore, the phenanthroline spectrophotometry method was used to determine the Fe^{2+}/Fe^{3+} concentration in the leachates with a spectrophotometer at 510 nm (721, China) [20]. The determination of the pH_{pzc} of the

Table 1
Chemical composition of the coal fly ash

Content	SiO_2	Al_2O_3	Fe_2O_3	CaO	TiO_2	Na_2O	SO_3	LOI
wt%	45.51	21.38	19.36	3.24	0.74	1.32	0.97	1.96

Note: LOI—loss on ignition.

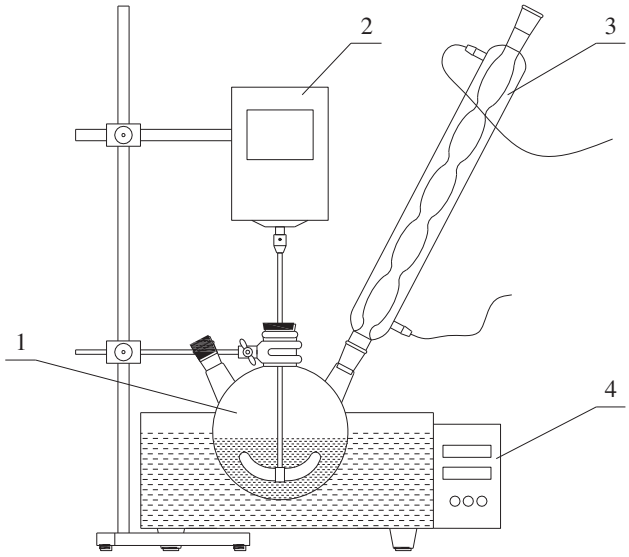

Fig. 1. Experimental setup. 1—Three-necked glass reactor, 2—stirrer, 3—condenser, and 4—water bath.

samples was carried out as follows [21]: 50 cm^3 of 0.01 M NaCl solution was placed in a closed Erlenmeyer flask. The pH was adjusted to a value between 2 and 12 by adding HCl 0.1 M or NaOH 0.1 M solutions. Then, 0.15 g of each coal fly ash sample was added and the final pH was measured after 48 h under agitation at room temperature. The pH_{pzc} is the point where the curve pH_{final} vs. $pH_{initial}$ crosses the line $pH_{initial} = pH_{final}$.

3. Experimental results and discussion

3.1. Effect of the sodium carbonate dosage

The acid leaching process is known to be sensitive to the dosage of the Na_2CO_3 activator. Different Na_2CO_3 dosages were mixed with 100 g of coal fly ash to activate the fly ash, and then the mixture was calcined. A 4 mol L^{-1} HCl solution was then used to leach the activated samples at 80 °C for 2 h. The effects of the Na_2CO_3 dosage on the Al^{3+} leaching rate are shown in Fig. 2. When the Na_2CO_3 dosage was lower

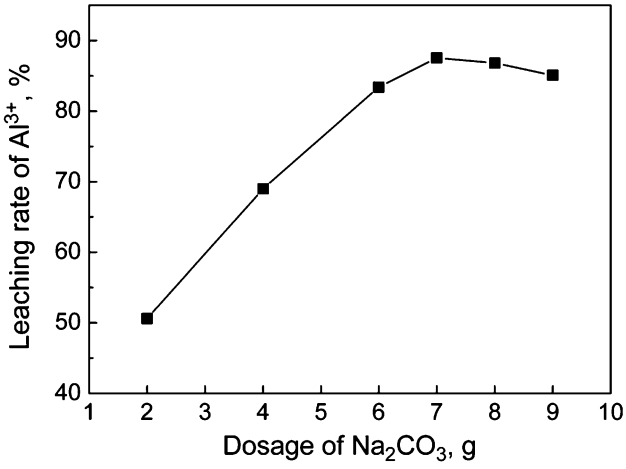

Fig. 2. Effect of the Na_2CO_3 dosage on the Al^{3+} leaching rate.

than 7 g, the Al^{3+} leaching rate increased as the dosage was increased. However, the Al^{3+} leaching rate decreased as the Na_2CO_3 dosage increased above 7 g. The maximum leaching rate was found when the mass ratio of the coal fly ash to the Na_2CO_3 was 100:7, and this shows that Na_2CO_3 had an important influence on the acid leaching process.

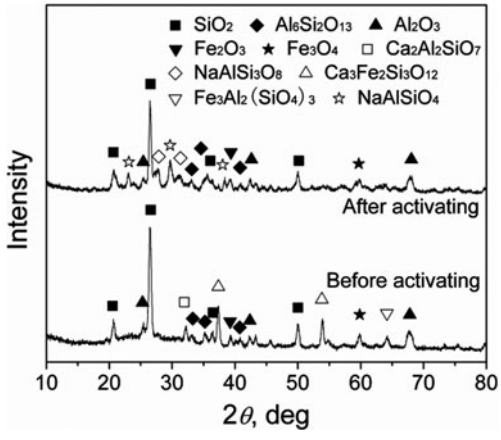

Fig. 3. X-ray diffraction patterns of the coal fly ash before and after activation.

The coal fly ash samples before and after activation were analyzed by X-ray diffraction to determine the effect of the Na_2CO_3, and the results are shown in Fig. 3. It can be seen that the raw fly ash sample was complex, and it contained many mineral phases, including SiO_2, $Al_6Si_2O_{13}$, Al_2O_3, Fe_2O_3, Fe_3O_4, $Ca_2Al_2SiO_7$, and $Ca_3Fe_2Si_3O_{12}$. Some glass phases were also found in the raw fly ash, but no sodium compounds were detected in this sample. Sodium compounds may not have been found in the raw fly ash sample because of the low Na_2O concentration in the fly ash, and the Na_2O that was present would have been dispersed in the mineral and glass phases. Several mineral phases disappeared when Na_2CO_3 was added to the fly ash and the mixture was sintered at 800°C, and the $NaAlSi_3O_8$ and $NaAlSiO_4$ phases, which were not found in the raw fly ash sample, appeared. This means that the Na_2CO_3 that was added reacted with the fly ash according to Eqs. (1) and (2) during the sintering process, and this could have broken the stable Si–Al bonds of the mullite phase, producing some soluble compounds that were easily leached by acid. This allowed most of the Al to be extracted from the coal fly ash (Eqs. (3) and (4)). There was an excess of Na_2CO_3 present at higher Na_2CO_3 dosages, and this excess could react with the nepheline that was generated in the system, producing the alkaline nepheline complex $(Na_2O)_{0.33}NaAlSiO_4$ [8], meaning that the active soluble aluminum compounds that were produced from the coal fly ash were turned back into an inert aluminum compound. This suggests that a Na_2CO_3 dosage of 7 g should be mixed with 100 g of coal fly ash to conserve the reagents and to improve the Al^{3+} leaching rate. The diffraction intensity of the Fe_2O_3 peak was enhanced when the fly ash was activated, as shown in Fig. 3, indicating that the Na_2CO_3 that was added increased the Fe^{2+}/Fe^{3+} leaching rate. Those results can also be proved by Fig. 4, which depicted that the concentration of Al^{3+} and Fe^{2+}/Fe^{3+} in the leachate of the activated fly ash sample is higher than that in the leachates of the raw fly ash sample.

$$3Al_2O_3 \cdot 2SiO_2 + 7SiO_2 + 6Na_2CO_3 \rightarrow 6NaAlSiO_4 + 3Na_2SiO_3 + 6CO_2 \uparrow \quad (1)$$

$$3Al_2O_3 \cdot 2SiO_2 + 9SiO_2 + 6Na_2CO_3 \rightarrow NaAlSi_3O_8 + 3Na_2SiO_3 + 6CO_2 \uparrow \quad (2)$$

$$NaAlSiO_4 + 4HCl \rightarrow AlCl_3 + NaCl + H_2SiO_3 + H_2O \quad (3)$$

$$NaAlSi_3O_8 + 4HCl \rightarrow AlCl_3 + NaCl + 3SiO_2 + 2H_2O \quad (4)$$

3.2. Effect of the HCl concentration

To investigate the effects of using different HCl concentrations on the acid leaching process, 7 g of Na_2CO_3 was mixed with 100 g coal fly ash when preparing the activated coal fly ash sample. The activated mixture was then leached using different HCl solutions (300 mL) at different concentrations at 80°C for 2 h. HCl concentrations of 1, 2, 4, and 6 mol L^{-1} were used. The effects of the HCl concentration on the Al^{3+} leaching rate are shown in Fig. 5. It can be seen that the HCl concentration played an important role in the acid leaching process, and increasing the HCl concentration increased the Al^{3+} leaching rate.

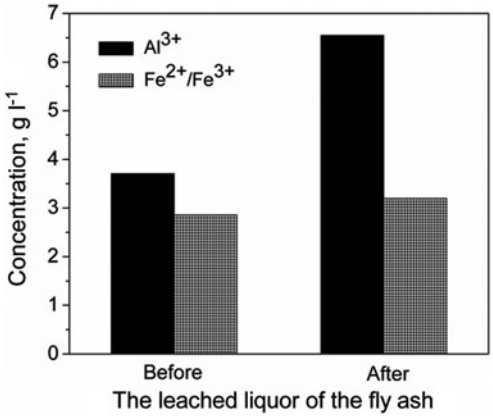

Fig. 4. Concentration of Al^{3+} and Fe^{2+}/Fe^{3+} in the leached liquor of the fly ash.

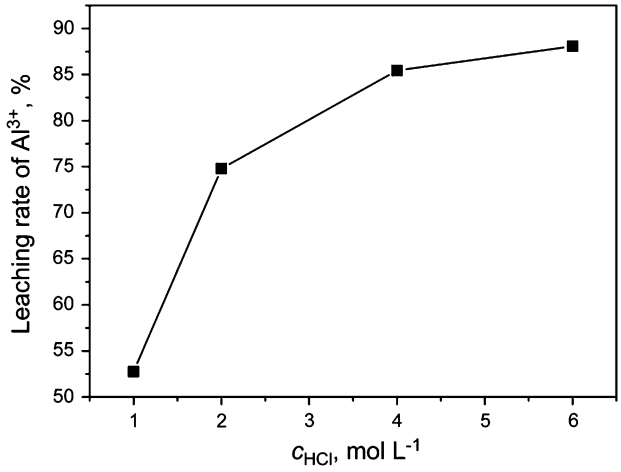

Fig. 5. Effect of the HCl concentration on the Al^{3+} leaching rate.

However, the Al^{3+} leaching rate continued to increase when the HCl concentration was increased from 4 to 6 mol L^{-1}, and a high HCl concentration could result in the reaction being too violent, leading to the loss of large amounts of volatile chemicals. Furthermore, using high HCl concentrations led to the suction filtration process being very difficult to perform, and this was possibly caused by the large amounts of aluminum-containing silica sol that was generated during the acid leaching process at these high HCl concentrations [12,22]. This means that using too high a HCl concentration not only increased the cost, but also had negative impacts on the leaching operation and environment. A HCl concentration of 4 mol L^{-1} was therefore chosen for the subsequent investigations, to give a reaction that would proceed completely.

3.3. Effect of the leaching time

The effects of the leaching time on the Al^{3+} leaching rate are shown in Fig. 6. An activated coal fly ash sample (7 g Na_2CO_3 and 100 g coal fly ash) was leached using 4 mol L^{-1} HCl (300 mL) at 80℃ for 0.5, 1, 1.5, 2, 2.5, and 3 h. It can be seen that the Al^{3+} leaching rate gradually increased as the leaching time was increased. However, the leaching rate had increased almost to its maximum at a leaching time of 2 h, then it tended to remain stable, and it started to decrease at a leaching time of 3 h. This was because the soluble aluminum compound concentration was constant, and these compounds could react with SiO_2, $Al_6Si_2O_{13}$, $NaAlSi_3O_8$, and $NaAlSiO_4$ in the activated coal fly ash at leaching times longer than 3 h, transforming the sodium aluminosilicate precipitate, which cannot react with HCl. This process is also a problem in the aluminum industry [23,24]. Moreover, a long leaching time increases the power consumed in the process. The acid leaching time used in the subsequent investigations was therefore 2 h, to achieve the optimum reaction efficiency.

3.4. Effect of the leaching temperature

The effects of the leaching temperature on the Al^{3+} leaching rate are shown in Fig. 7. The activated coal fly ash sample (7 g Na_2CO_3 and 100 g coal fly ash) was leached for 2 h using 4 mol L^{-1} HCl (300 mL) at 60, 70, 80, 90, 100, and 110℃. The Al^{3+} leaching rate increased noticeably as the acid leaching temperature was increased, which is completely in accordance with the classical theory of chemical reaction kinetics (i.e. that an increase in temperature speeds up a reaction) [25]. The obvious reaction phase lasted for 30 and 12 min when the leaching temperature was 60 and 80℃, respectively. Increasing the leaching temperature to 110℃ impaired the condensation and reflux processes, resulting in the noticeable volatilization of HCl. This caused the HCl concentration to decrease to a large extent, leading to the Al^{3+} leaching rate eventually decreasing. This shows that using too high a leaching temperature wastes energy resources and cause the volatilization of large amounts of HCl, which will not only pollute the environment and harm human health, but decrease the Al^{3+} leaching rate. The acid leaching temperature should, therefore, be strictly controlled to ensure that the reaction can proceed. We thought that the leaching temperature should be within the range 80–100℃ in the subsequent investigations, so three temperatures, 80, 90, and 100℃, were selected for use when optimizing the experimental conditions in the orthogonal test.

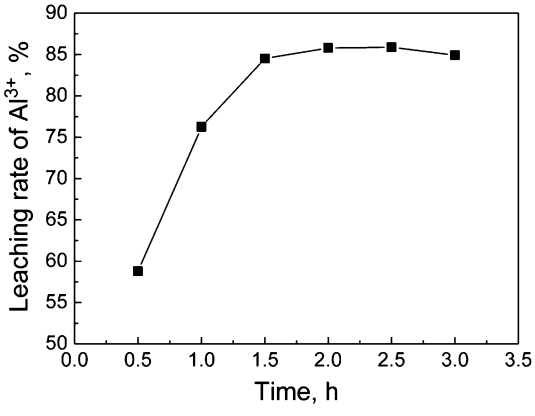

Fig. 6. Effect of the leaching time on the Al^{3+} leaching rate.

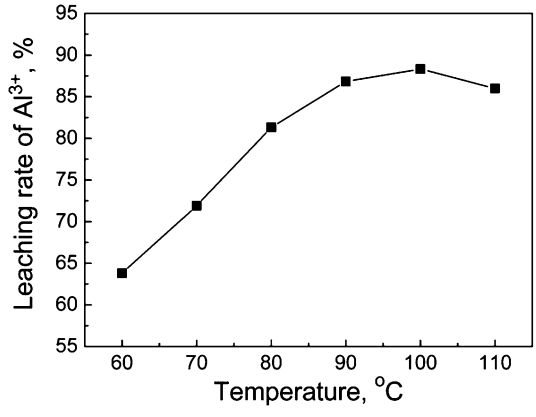

Fig. 7. Effect of the leaching temperature on the Al^{3+} leaching rate.

3.5. Optimization of the experiment conditions for acid leaching coal fly ash

An orthogonal test was performed to optimize the acid leaching process conditions, and four factors, each at three levels, were chosen, based on the results of previous research and qualitative experiments. The matrix experiment was designed by selecting the appropriate orthogonal $L_9(3^4)$ array for the control parameters. The controlled factors and their levels that were used in the $L_9(3^4)$ array are presented in Table 2. The matrix experiments were conducted, and the Al^{3+} leaching rate was used as the experimental response. The results are shown in Table 3.

The best conditions that were found, seen in Table 3, were 6 g Na_2CO_3 in 100 g fly ash, 4 mol L^{-1} HCl, a 1.5 h leaching time, and a temperature of 90˚C. These conditions gave an Al^{3+} leaching rate of 90.36%.

Visual analysis of the orthogonal test results is an important method of evaluating the controllable factors and their levels, and this can allow the controllable factors to be put into an appropriate order of importance and allow optimal combinations of the levels to be selected [26]. Table 4 shows the total response K, average response k, and range R for each factor calculated at each level. For example, the total response to factor B at level 2 was calculated as $K_2 = (L_2 + L_5 + L_8)$, L_2 is the leaching rate for run no. 2, the average response to factor B at level 2 was calculated as $k_2 = (L_2 + L_5 + L_8)/3$, and R is the maximum k value for each factor minus the minimum k value. The k value can provide the optimal level for the design parameters giving the greatest k,

Table 4
Visual analysis of the orthogonal test results

	A	*B*	*C*	*D*
K_1	259.23	242.12	246.49	251.92
K_2	253.41	258.55	258.25	252.35
K_3	244.66	256.63	252.56	253.03
k_1	86.41	80.71	82.16	83.23
k_2	84.47	86.18	86.08	84.12
k_3	81.55	85.54	84.19	84.34
R	4.86	5.47	3.92	1.11
Optimal	A_1	B_2	C_2	D_3

Table 2
Factors and levels used in the orthogonal test

	Factor			
Level	Dosage of $NaCO_3$ (g) *A*	HCl concentration (mol L^{-1}) *B*	Acid leaching time (h) *C*	Acid leaching temperature (˚C) *D*
1	6	2	1.0	80
2	7	4	1.5	90
3	8	6	2.0	100

Table 3
$L_9(3^4)$ orthogonal table and the test results

	Factor				Response
Run no.	Dosage of $NaCO_3$ (g) *A*	HCl concentration (mol L^{-1}) *B*	Acid leaching time (h) *C*	Acid leaching temperature (˚C) *D*	Leaching rate (%)
1	6	2	1.0	80	80.82
2	6	4	1.5	90	90.36
3	6	6	2.0	100	88.05
4	7	2	1.5	100	83.17
5	7	4	2.0	80	86.38
6	7	6	1.0	90	83.86
7	8	2	2.0	90	78.13
8	8	4	1.0	100	81.81
9	8	6	1.5	80	84.72

and the R value can provide the order of importance for the controllable factors [26]. From Table 4, it can be seen that the importance of the factors decreased in the order HCl concentration > Na_2CO_3 dosage > acid leaching temperature > acid leaching time. The values A_1 (6 g Na_2CO_3 in 100 g fly ash), B_2 (4 mol L^{-1} HCl), C_2 (1.5 h), and D_3 (100˚C) were found to be the optimal parameter levels for the acid leaching of coal fly ash. The optimal conditions gave an Al^{3+} leaching rate of 90.68% and Al^{3+} and Fe^{2+} plus Fe^{3+} concentrations in the leaching liquid of 34.21 and 30.67 g L^{-1}, respectively.

3.6. Comparison of the coal fly ash before and after acid leaching

Fig. 8 shows SEM images of the coal fly ash samples before and after acid leaching. As compared with Fig. 8(a) and (b) displays that the HCl treatment changed the surface structures of the initial ash microspheres, and the treated particles displayed flakes, folding flakes, and porous structures, and the edges and corners became sharper. There were clear traces of erosion on the surfaces, and the surfaces became rough after HCl treatment, implying that Al and Fe elements were leached by HCl, and that the specific surface area of the ash had been increased noticeably by the leaching process.

Fig. 9 and Table 5 show the EDS data for the coal fly ash samples before and after acid leaching. Although the relative amounts of the components can be inferred from their relative peak heights, the intensities of the peaks in the EDS are not quantitative measures of the elemental concentration, but are only semi-quantitative measures [27]. We found that Si, Al, and Fe were the major constituents, and this is consistent with the elemental compositions determined by XRF. The very high C concentrations in the ash samples indicate that incomplete and poor combustion of the coal occurred in the power plant. The elements O, Na, Mo, K, and Ca were found in the initial ash sample, and the Al, Ca, and Na concentrations were noticeably lower in the leached ash than in the initial ash. This indicates that there were considerable losses of metal ions during the acid leaching process, and this could have caused the specific surface area of the leached ash sample to be higher than the specific surface area of the initial ash sample. Table 5 shows that the Fe concentration was higher in the leached ash sample than in the initial ash sample, even though Fe^{2+} and Fe^{3+} were found at measurable concentrations in the leaching liquid. This apparent contradiction occurred because the data listed in Table 5 are the relative contents, and the leaching of

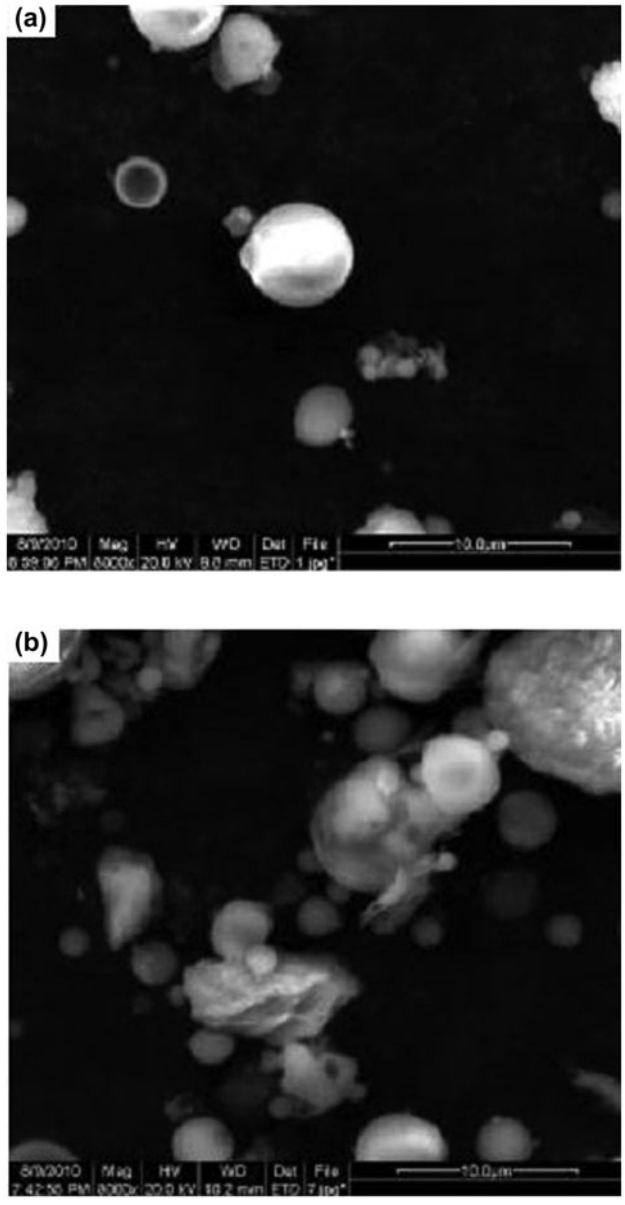

Fig. 8. SEM images of the coal fly ash (a) before and (b) after leaching.

Al, Ca, Na, and other elements will have led to the relative contents of other elements present in the leached ash to increase. This also suggests that there was still a considerable amount of Fe in the leached ash that had not been leached.

The specific surface area of the ash and the pore size distribution in the ash were determined from N_2 adsorption–desorption isotherms, and the specific surface area of the coal fly ash was calculated using the BET equation. The BET analysis showed that the specific surface area in the initial ash was 24.50 m^2

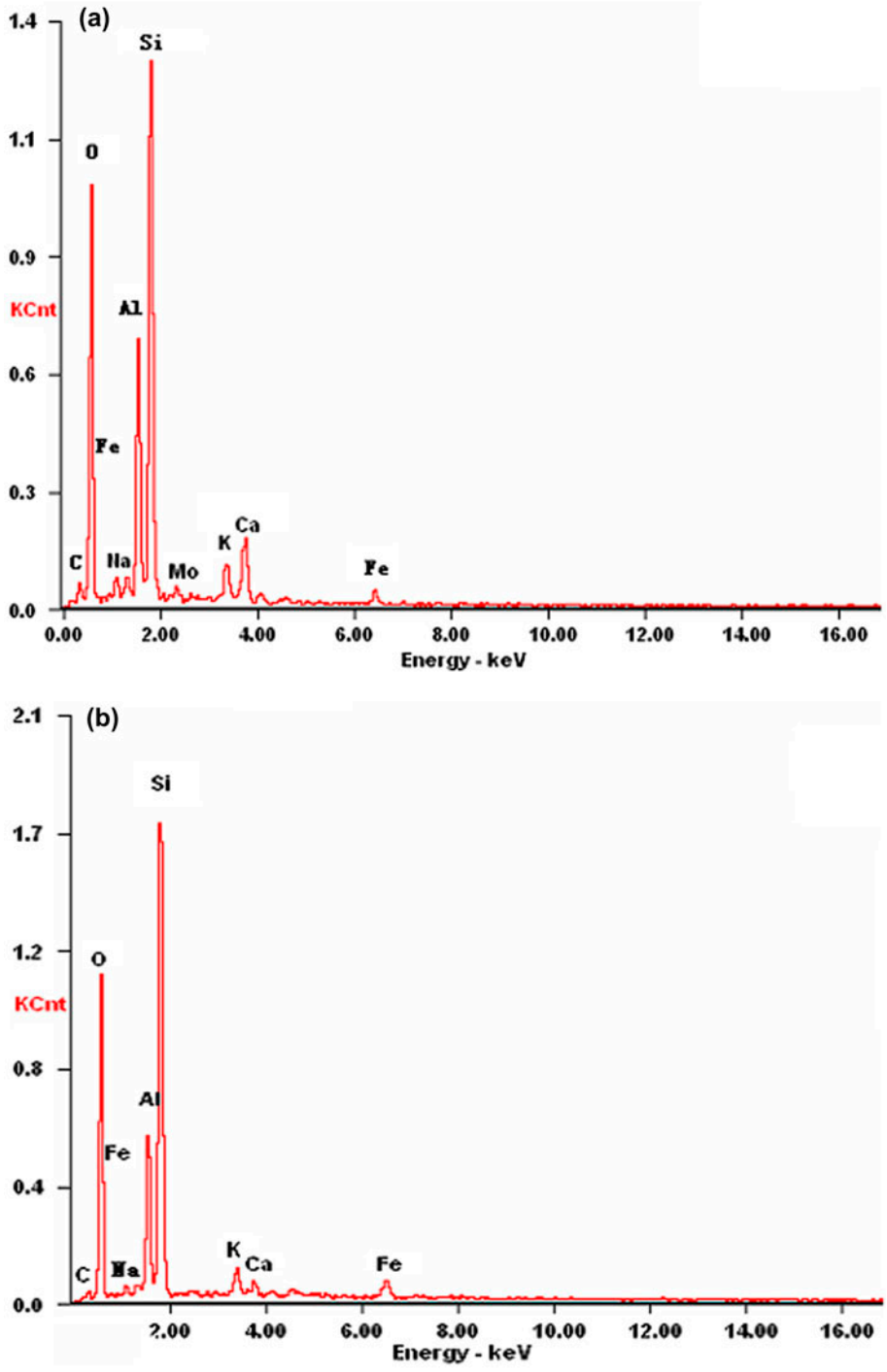

Fig. 9. EDS of the coal fly ash (a) before and (b) after leaching.

g^{-1}, the pore volume was 0.01 g^{-1} cm^3, and the average pore diameter was 2.5 nm, and that these parameters increased to 55.73 m^2 g^{-1}, 0.03 g^{-1} cm^3, and 2.9 nm, respectively, when the coal fly ash had been leached. The increases in these parameters were related to the leaching of certain components during the acid treatment, but the low specific surface area and small pore volume of the initial ash with a relatively large mean pore radius indicated that the ash contained mesopores (pore radii of 1–25 nm) and

Table 5
Elemental contents of the coal fly ash before and after leaching

	Element	C	O	Na	Al	Si	Mo	K	Ca	Fe
Before leaching	wt%	8.70	41.16	1.5	13.24	17.87	1.97	1.95	2.38	11.23
	at%	13.77	50.68	1.24	9.31	12.11	0.39	0.95	1.13	10.42
After leaching	wt%	1.27	36.36	0.79	9.55	32.45	–	2.99	1.66	14.93
	at%	0.75	51.87	0.73	7.52	24.78	–	1.62	0.88	11.87

Notes: wt% = weight percentage.
at% = percentage by numbers of atoms.

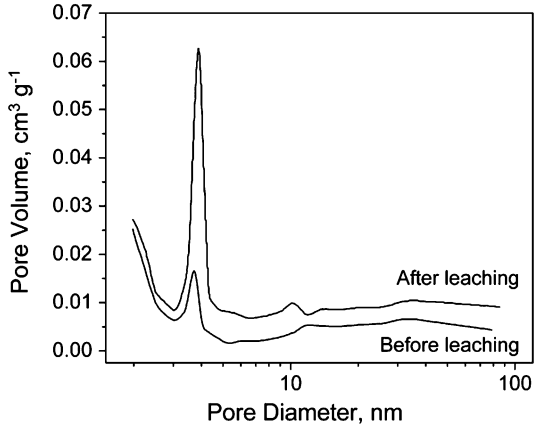

Fig. 10. Pore distribution in the coal fly ash before and after leaching.

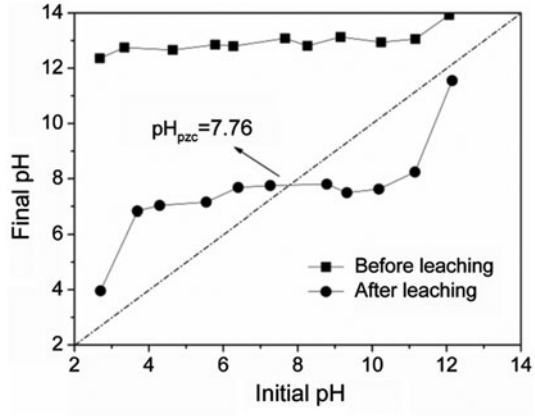

Fig. 12. Determination of pH_{pzc} of the coal fly ash before and after leaching.

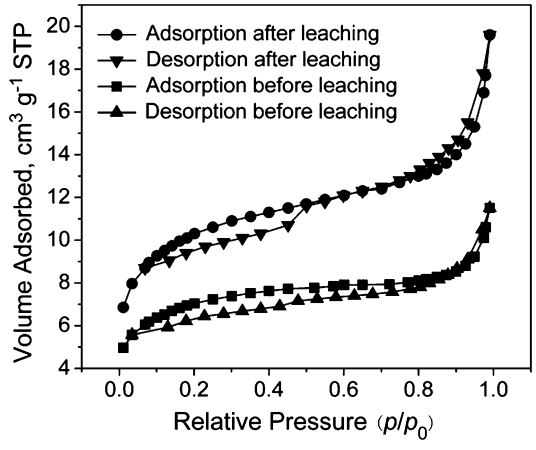

Fig. 11. N_2 adsorption–desorption isotherms for the coal fly ash before and after leaching.

macropores (pore radii > 25 nm), according to the IUPAC classification system [28]. This supposition was confirmed by the dependence of the adsorbed nitrogen volume on the pore radius (Fig. 10). The dominant pores had radii of 2–3 nm in the initial ash. A similar conclusion was drawn for the leached ash, in which mesopores with radii 2–3 nm were abundant, and a contribution from mesopores with radii of 10 nm was also established. The pore volumes of the mesopores and macropores were found to be higher in the leached ash than in the initial ash, as is shown in Fig. 10. This again proved to be a consequence of the extraction of the soluble components of the fly ash into the leaching liquid.

The nitrogen adsorption isotherm for the initial ash (Fig. 11) was classified as type II in the IUPAC classification [28]. This kind of isotherm corresponds to a situation when a monolayer of nitrogen is formed at relatively low pressures and a nitrogen multilayer is formed at relatively high pressures. This characteristic is typical of mesoporous materials. The small specific surface area and low pore volume with a relatively large mean pore radius indicates that the fly ash that was tested had a macroporous structure. The fact that the hysteresis loop finished at a relatively high pressure also implied that there was a contribution from macropores. The hysteresis loop was classified as the H2 type with an admixture of the H4 type [29], which

means that the pore structure was overwhelmingly formed by spherical or granular crystals.

The leached fly ash sample gave different nitrogen adsorption isotherm characteristics, as is shown in Fig. 11. Adsorption by the leached fly ash increased noticeably at relatively high pressures, which means that the number of mesopores and macropores was much higher in this sample than in the initial ash sample. The isotherm was classified as type I with an admixture of type II, which corresponds to a mesoporous adsorbent (like zeolite-like crystalline solids) containing some macropores [28]. The hysteresis loop looked like that of an admixture of type H2 and type H3, and this characteristic is associated with a varied pore structure containing networks and channels [30], which is consistent with the increase in the pore size distribution and the specific surface area that occurred through the leaching process. These results also correspond with the results of the SEM and EDS analyses.

Fig. 12 depicted the results of "pH drift" experiment, from which the pH_{pzc} of the initial coal fly ash sample was not found, and its surface has a basic character. However, the pH_{pzc} of the leached fly ash sample in this test was found to be 7.76, this means that pH_{pzc} of the coal fly ash was influenced by the chemical composition, mainly composed of SiO_2, Al_2O_3, and Fe_2O_3 [31]. The leached fly ash sample is material with amphoteric character after Al and Fe elements were leached by HCl, thus, depending on the pH of the solution, their surfaces might be positively or negatively charged. At $pH < pH_{pzc}$, the leached fly ash surface becomes positively charged favoring the adsorption of anionic species. On the other hand, adsorption of cationic species will be favored at $pH > pH_{pzc}$ [32].

3.7. Analysis of the cost and environmental effect

Overall, the leached residue of coal fly ash can be transformed to an adsorbent. Lots of coal fly ash and excess hydrochloric acid are produced in Yulin power plants and chlor-alkali chemical plants because Yulin City is an important energy and chemical industries base in China, the price is about 0–26 and 100–200 RMB/t, respectively. Furthermore, the waste heat from power plant may be utilized for the reaction required, the transportation cost of these local raw materials can be saved, the leachate can also be used to produce a coagulant, this means that comprehensive utilization of local resources and coal solid wastes is feasible from the perspective of environmental protection and sustainable energy development, good effect and low cost can be obtained in the leaching coal fly ash process.

4. Conclusions

The optimal conditions for the acid leaching of coal fly ash were investigated by determining the effects of the controllable factors and using an orthogonal test. The coal fly ash before and after leaching was also analyzed using SEM, EDS, and BET analysis. The specific surface area, the pore volume, and the average pore diameter were higher in the leached ash sample than in the initial ash, and this was caused by the leaching of some of the coal fly ash components during the acid treatment.

Acknowledgments

This work was sponsored in part by National Natural Science Foundation of China (21203163), Science and Technology Plan Project of Yulin Government (Sf13-09, Gy1309), Shaanxi Provincial Education Department (2013JK0686) and Scientific Research Project of Yulin University (12GK03, 11GK36).

References

[1] R. Zhai, P. Peng, Y. Yang, M. Zhao, Optimization study of integration strategies in solar aided coal-fired power generation system, Renew. Energy 68 (2014) 80–86.
[2] Y. Yang, X. Guo, N. Wang, Power generation from pulverized coal in China, Energy 11 (2010) 4336–4348.
[3] H. Liu, Z. Liu, Recycling utilization patterns of coal mining waste in China, Resour. Conserv. Recycl. 54 (2010) 1331–1340.
[4] Z. Bian, J. Dong, S. Lei, H. Leng, S. Mu, H. Wang, The impact of disposal and treatment of coal mining wastes on environment and farmland, Environ. Geol. 58 (2009) 625–634.
[5] S. Wang, Application of solid ash based catalysts in heterogeneous catalysis, Environ. Sci. Technol. 42 (2008) 7055–7063.
[6] M. Ahmaruzzaman, A review on the utilization of fly ash, Prog. Energy Combust. Sci. 36 (2010) 327–363.
[7] S. Dai, L. Zhao, S. Peng, C. Chou, X. Wang, Y. Zhang, D. Li, Y. Sun, Abundances and distribution of minerals and elements in high-alumina coal fly ash from the Jungar Power Plant, Inner Mongolia, China, Int. J. Coal Geol. 81 (2010) 320–332.
[8] Y. Guo, Y. Li, F. Cheng, M. Wang, X. Wang, Role of additives in improved thermal activation of coal fly ash for alumina extraction, Fuel Process. Technol. 110 (2013) 114–121.
[9] J.H. Brindle, M.J. McCarthy, Chemical constraints on fly ash glass compositions, Energy Fuels 20 (2006) 2580–2585.
[10] L. Yan, Y. Wang, H. Ma, Z. Han, Q. Zhang, Y. Chen, Feasibility of fly ash-based composite coagulant for coal washing wastewater treatment, J. Hazard. Mater. 203–204 (2012) 221–228.

[11] T. Sun, C. Sun, G. Zhu, X. Miao, C. Wu, S. Lv, W. Li, Preparation and coagulation performance of poly-ferric-aluminum-silicate-sulfate from fly ash, Desalination 268 (2011) 270–275.
[12] M. Visa, L. Isac, A. Duta, Fly ash adsorbents for multi-cation wastewater treatment, Appl. Surf. Sci. 258 (2012) 6345–6352.
[13] M. Ahmaruzzaman, Role of fly ash in the removal of organic pollutants from wastewater, Energy Fuels 23 (2009) 1494–1511.
[14] E.J. Reardon, C.A. Czank, C.J. Warren, R. Dayal, H.M. Johnston, Determining controls on element concentrations in fly ash leachate, Waste Manage. Res. 13 (1995) 435–450.
[15] T. Praharaj, M.A. Powell, B.R. Hart, S. Tripathy, Leachability of elements from sub-bituminous coal fly ash from India, Environ. Int. 27 (2002) 609–615.
[16] B. Cetin, A.H. Aydilek, Y. Guney, Leaching of trace metals from high carbon fly ash stabilized highway base layers, Resour. Conserv. Recycl. 58 (2012) 8–17.
[17] S. Wang, Y. Boyjoo, A. Choueib, Z.H. Zhu, Removal of dyes from aqueous solution using fly ash and red mud, Water Res. 39 (2005) 129–138.
[18] Y.Q. Li, Preparation of Coagulant from Fly Ash and its Application in Coagulation Constructed Wetland (Dissertation for the Doctoral Degree), Harbin Institute of Technology, 2008, (in Chinese).
[19] The State Administration of China Quality Supervision Inspection and Quarantine, GB15892-2003, Water Treatment Chemical—Poly Aluminium Chloride 2003-06-03.
[20] State Environmental Protection Administration, HJ/T 345-2007, Water Quality-Determination of Iron-Phenanthroline Spectrophotometry, 2007-03-10.
[21] J. Rivera-Utrilla, I. Bautista-Toledo, M.A. Ferro-García, C. Moreno-Castilla, Activated carbon surface modifications by adsorption of bacteria and their effect on aqueous lead adsorption, J. Chem. Technol. Biotechnol. 76 (2001) 1209–1215.
[22] R.S. Blissett, N.A. Rowson, A review of the multi-component utilisation of coal fly ash review article, Fuel 97 (2012) 1–23.
[23] A.A. Landman, Data reduction, and cluster and discriminant analysis of aluminosilicate infrared spectra—Fly ash reacted at 860 C with sodium carbonate as a model system, Vib. Spectrosc. 37 (2005) 209–216.
[24] M. Liu, L. Hou, B. Xi, Y. Zhao, X. Xia, Synthesis, characterization, and mercury adsorption properties of hybrid mesoporous aluminosilicate sieve prepared with fly ash, Appl. Surf. Sci. 273 (2013) 706–716.
[25] Beijing Normal University, Central China Normal University, Nanjing Normal University, Inorganic Chemistry, third ed., Higher Education Press, Beijing, 1992.
[26] Q. Zhuo, H. Ma, B. Wang, F. Fan, Degradation of methylene blue: Optimization of operating condition through a statistical technique and environmental estimate of the treated wastewater, J. Hazard. Mater. 153 (2008) 44–51.
[27] B.G. Kutchko, A.G. Kim, Fly ash characterization by SEM–EDS, Fuel 85 (2006) 2537–2544.
[28] K.S.W. Sing, D.H. Everett, R.A.W. Haul, L. Moscou, R.A. Pierotti, J. Rouquerol, T. Siemieniewska, Reporting physisorption data for gas/solid systems with special reference to the determination of surface area and porosity, Pure Appl. Chem. 57 (1985) 603–619.
[29] S.W. Kenneth, R.T. Williams, Physisorption hysteresis loops and the characterization of nanoporous materials, Adsorpt. Sci. Technol. 22 (2004) 773–782.
[30] J. Rouquerol, D. Avnir, C.W. Fairbridge, D.H. Everett, J.H. Haynes, N. Pernicone, J.D.F. Ramsay, K.S.W. Sing, K.K. Unger, Recommendations for the characterization of porous solids, Pure Appl. Chem. 66 (1994) 1739–1758.
[31] D. Sun, X. Zhang, Y. Wu, X. Liu, Adsorption of anionic dyes from aqueous solution on fly ash, J. Hazard. Mater. 181 (2010) 335–342.
[32] P.C.C. Faria, J.J.M. Órfão, M.F.R. Pereira, Adsorption of anionic and cationic dyes on activated carbons with different surface chemistries, Water Res. 38 (2004) 2043–2052.